



XP 000400013

8272 IEEE Journal on Selected Areas in  
Communications  
11(1993) September, No. 7, New York, US

3, SEPTEMBER 1993

H04L25/30V

# A Soft-Output Bidirectional Decision Feedback Equalization Technique for TDMA Cellular Radio

H04B7/005

p.1034-1045

Yow-Jong Liu, Member, IEEE, Mark Wallace, and John W. Ketchum

**Abstract**—Issues encountered in the design of reliable narrowband TDMA digital cellular mobile communication systems are considered. In particular, the problem of compensating for the harsh multipath fading environment in systems whose transmission bandwidth is commensurate with the coherence bandwidth of the fading channel is considered.

A new TDMA channel characterization parameter, the slot-normalized fade rate, is introduced and a novel adaptive bidirectional equalization technique, which is able to estimate the location of a deep fade within a time slot, is proposed. The simulation results show that the carrier-to-noise ratio requirement is only 15.5 dB when this equalization technique is used. This is achieved without diversity, and with low complexity. This is also 6.5 dB lower than called for in the IS-54 specification, which requires 3% BER at  $E_b/N_0$  equal to 22 dB and vehicle speed equal to 60 mph under certain channel conditions.

An equivalent equalized land/mobile radio channel model and the analytical solution for the optimal bit likelihood calculation for  $\pi/4$ -shift QDPSK modulation are also derived under certain channel conditions. The results are used as soft decisions for the convolutional decoder. The likelihood calculation requires an estimate of the instantaneous noise variance. A good estimate may be derived from the equalizer error signal, but care must be taken to avoid use of the error signal when the equalizer is not tracking the channel. This approach gives a 1% decoded BER with 2 dB less power than that required for hard decisions.

## I. INTRODUCTION

SUCCESSFUL deployment of first-generation digital cellular systems in North America depends on the development of high-performance digital communication techniques for reliable operation in the hostile fading and interference environments typical of mobile and cellular systems. These techniques must also meet the reasonable complexity/performance tradeoffs that must be made in the system design stages of these developments. Several different system design and multiple access approaches are under consideration and/or development by various organizations. These techniques include time division multiple access (TDMA) [1], [2] and spread spectrum code division multiple access (SS/CDMA) [3].

This paper considers the case of a narrowband TDMA system, which is under development as a standard, IS-54, for North American Digital Cellular technology [2]. It has been shown that the system performance can be significantly

improved by using diversity reception techniques [4]. The results also indicate that only 13.5 dB of signal-to-noise power ratio is required to achieve 3% BER at a vehicle speed equal to 60 mph, which is 8.5 dB lower than the IS-54 specification. Therefore, the reverse link (from mobile to base station) performance requirement specified in the standard can easily be achieved by the receivers with diversity reception at the base station.

However, diversity reception, using either space or antenna diversity techniques, will increase the complexity of the receiver front end. In order to minimize the complexity of the hand-held units, different approaches should be used to improve the receiver sensitivity. It is the purpose of this paper to investigate the performance of the forward link (from base station to mobile station) under the assumption of no-diversity reception and to address some design issues encountered in the receivers.

In this paper, we first introduce a new channel characteristic index for TDMA systems called the *slot-normalized fade rate*. This index represents the average number of occurrences of fades per time slot. A novel bidirectional adaptive equalization technique, which takes advantage of the periodic transmission of training bits in the TDMA frame structure to estimate the location of a deep fade within a time slot, is then proposed. The major difference between our approach and conventional techniques is that an additional control mechanism is added to monitor the error signal providing information on the tracking status of the equalizer [5].

We have also derived an equivalent model which encompasses the bidirectional equalizer and the frequency-selective fading mobile radio channel. The maximum likelihood metric is then derived for this channel, generating soft-decision metrics for the decoder, and  $\pi/4$ -shift QDPSK modulation. We show that the error signal from the equalizer may be used to derive an estimate of the instantaneous SNR, which is required for the calculation of these metrics. The resulting soft decisions provide a decoded BER of 1% with 2 dB less power than that required for hard decisions.

The paper is organized as follows. Section II describes the system model used in this study. Section III introduces the new index, the slot-normalized fade rate. Section IV reviews previous equalization techniques and describes in detail the proposed technique. Section V derives the equivalent bidirectional equalized radio channel and soft-decision metrics

Manuscript received March 1992; revised December 1992. This paper was presented at IEEE GLOBECOM '91, Phoenix, AZ.

The authors are with the Mobile Systems Department, GTE Laboratories Inc., Waltham, MA 02254.

IEEE Log Number 9210925.

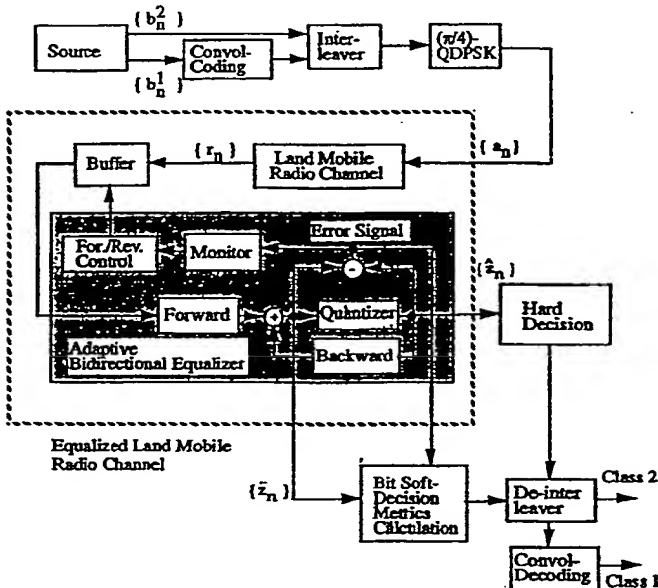


Fig. 1. Simplified system diagram.

for the decoder and complete IS-54 link simulation results. Finally, the conclusions of this study are given in Section VI.

## II. SYSTEM DESCRIPTION

The block diagram of the simplified digital communication system under study is shown in Fig. 1. The output sequence from the source is divided into two classes. Class 1 bits, denoted by  $b^1 = (b_1^1, \dots, b_n^1, \dots)$ , are protected by a convolutional code. Class 2 bits, denoted by  $b^2 = (b_1^2, \dots, b_n^2, \dots)$ , are not protected. These two binary sequences are passed to an interleaver with some finite interleaving span and depth. After interleaving, the data sequence is first modulated by a  $\pi/4$ -shift QDPSK. The modulated symbol sequence, denoted by  $a = (a_1, \dots, a_n, \dots)$ , is then transmitted through the land mobile radio channels.

Assuming perfect synchronization and coherent detection at the base station, the received symbol sequence  $\{r_n\}$  can be written as

$$r_n = \sum_{m=0}^L h_{m,n} a_{n-m} + \eta_n, \quad n \geq 0 \quad (1)$$

where  $h_{m,n}$ ,  $1 \leq m \leq L$ ,  $n \geq 0$  are  $L$  zero-mean discrete-time complex Gaussian random processes, uncorrelated in  $m$  but generally correlated in  $n$ . The autocorrelation function for each random process  $h_m$  is given by [6]

$$R(\tau) = AJ_0(2\pi f_D \tau) \quad (2)$$

where  $A$  is some normalized constant and  $f_D$  is the maximum Doppler frequency, determined by the maximum vehicle speed and carrier frequency.

All the received symbols in the current *effective time slot*<sup>1</sup> are first stored in a temporary buffer and then processed by

<sup>1</sup>An effective time slot contains all the training data symbols in the current time slot and only the training symbols in the adjacent time slot.

TABLE I  
EQUALIZER DESIGN PARAMETERS FOR GSM  
AND IS-54 DIGITAL CELLULAR STANDARD

System	$N_s$	$T_s$	$f_D$	$\gamma = f_D T_s$	$\kappa = f_D T_{\text{slot}}$
GSM	156.25	$3.692 \mu\text{sec}$	$100 \text{ Hz}$	0.000369	0.0577
IS-54	162	$41.5 \mu\text{sec}$	$80 \text{ Hz}$	0.0033	0.5333

the adaptive equalizer (the shaded area in the figure). Each functional block inside the adaptive equalizer will be discussed later in Section IV.

Class 2 bits  $b^2 = (b_1^2, \dots, b_n^2, \dots)$  are recovered, based on hard decisions, directly from the quantized outputs of the equalizer while Class 1 bits  $b^1 = (b_1^1, \dots, b_n^1, \dots)$  are recovered after the Viterbi decoder processes all the deinterleaved soft-decision metrics. The detailed derivation of soft-decision metrics will be discussed later in Section V.

## III. SYMBOL-NORMALIZED AND SLOT-NORMALIZED FADE RATES

A useful index of the rate at which the mobile radio channel varies with time is the *symbol-normalized fade rate*  $\gamma = f_D T_s$ , where  $f_D$  is the maximum Doppler frequency and  $T_s$  is the inverse of the channel symbol transmission rate. This index provides a convenient indication of the extent to which the channel can be considered to be stationary over a symbol interval.

In a channel structure which incorporates periodic transmission of training bits,  $\gamma$  is an incomplete measure of the rate at which the channel varies. For the training bits to be used effectively by the equalizer, they must be repeated sufficiently often relative to the fade rate to keep the equalizer tracking error small. To capture this requirement, a new fading channel index, the *slot-normalized fade rate*, is defined as

$$\kappa = f_D T_{\text{slot}} = N_s f_D T_s \quad (3)$$

where  $T_{\text{slot}}$  is the slot duration and  $N_s$  is the number of symbols per time slot. This number represents the rough average number of occurrences of deep fades per time slot.

Table I shows the value of  $\kappa$  and some other specifications for two proposed digital cellular standards: the Groupe Spéciale Mobile (GSM) Pan-European Digital Cellular Radio System [1], and the Telecommunications Industry Association (TIA) North American Digital Cellular Standard (IS-54) [2]. The vehicle speed is assumed to be 60 mph.

Based on the values of  $\gamma$  and  $\kappa$  listed in Table I, it is apparent that the relative time variations of the channel in the GSM system are much slower than for the IS-54 standard. The equalizer in the GSM system will face many fewer deep fades per time slot than the one used in the IS-54 Standard. Further, IS-54 requires adaptive algorithms with better tracking capability than those used in the GSM.

Fig. 2 shows the simulated BER performance of a conventional fast adaptive decision feedback equalizer [7] for different slot-normalized fade rates and two different symbol-normalized fade rates {0.0033, 0.00165}. System performance is first decided by the symbol-normalized fade rate  $\gamma$ . For a given fade rate, however, TDMA systems with the shortest

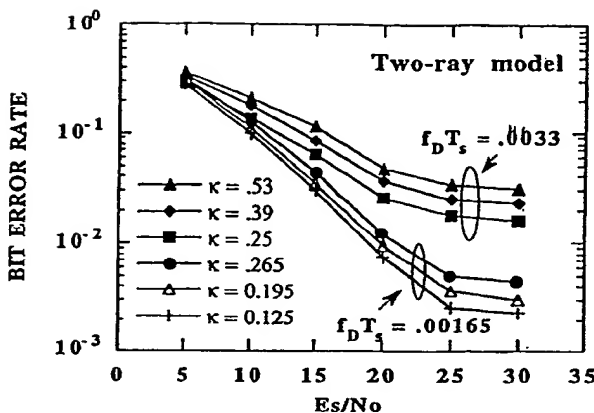


Fig. 2. BER as a function of fade rates and slot-normalized fade rate.

time slot or the smallest  $\kappa$  give the best performance. We conclude that both parameters,  $\gamma$  and  $\kappa$ , should be kept as small as possible in the design of a TDMA frame structure.

#### IV. ADAPTIVE EQUALIZATION TECHNIQUES

Adaptive equalization techniques have been extensively studied for application to time-varying radio channels subject to time-dispersive multipath propagation. One commonly used structure is the decision feedback equalization technique (DFE) (see, e.g., [7], [8]). The maximum likelihood sequence estimation (MLSE) approach using Viterbi algorithms is another effective way to compensate for the time-dispersive nature of the channel [9]–[11]. By substituting the Viterbi algorithm with the  $M$ -algorithm (a suboptimal tree search algorithm), the complexity of the MLSE equalizer can be substantially reduced at the expense of some performance degradation [12], [13].

##### A. One-Directional Equalization Techniques

Most previously proposed adaptive equalizers share a common characteristic in operating on received data, namely *one-directional equalization*. In general, a one-directional equalization procedure, which is shown in Fig. 3, is divided into two phases.

- 1) *Training Mode:* A sequence of training data which is known to the receiver is first used to help the equalizer to converge. In this mode, the equalizer also learns the trend of the channel variation.
- 2) *Tracking Mode:* A sequence of noisy and distorted user data, which must be recovered by the receiver, is then processed by the equalizer. In this mode, the equalizer also needs to track the channel variation.

In general, a portion of the time slot is allocated to the training symbol sequence. Two one-directional equalization procedures that are found in the existing literature are distinguished by the location of the training symbol sequence in the time slot.

- Training symbols at the beginning of each time slot, as shown in Fig. 3, have two possible equalization procedures:

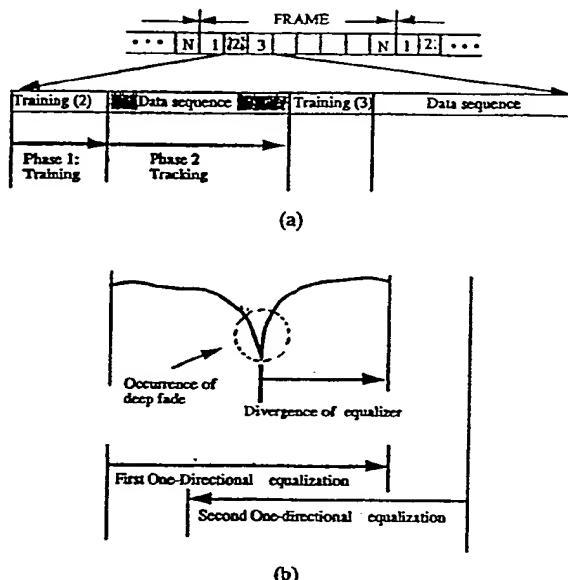


Fig. 3. Equalization procedure for TDMA communication systems with training symbols at the beginning of the time slot. (a) Single one-directional equalization. (b) Dual one-directional equalization.

- 1) *One-directional equalization:* Equalization is accomplished in a single pass, operating on the samples of the received waveform in sequence.
- 2) *Dual one-directional equalization:* Equalization is accomplished in two passes, operating on the received samples both in their original sequence and in reverse time, starting with the last sample and working toward the first. The output of the equalizer is chosen as the result of the pass with lower error signal. This scheme has also been referred to as the bidirectional equalization technique in [15], [16].
- Training symbols at the middle of each time slot, as shown in Fig. 4. Here the equalizer works in normal sequence, from the training bits to the end of the slot, and in reverse time from the training bits to the beginning of the block. In this approach, the effective slot-normalized fade rate is reduced by a factor of two since the equalizer is effectively only equalizing half the time slot for each use of the training sequence. As a result, the average number of deep fades per effective time slot is also reduced by a factor of two.

None of the previously proposed equalization techniques is able to estimate the location of a deep fade and, therefore, cannot recover data after a deep fade. As shown in Fig. 3, the occurrence of a deep fade located in the middle of user data will cause the divergence of the equalizer, since either there is no signal available to guide the adaptation algorithm or the channel variation is too fast for the adaptive equalizer to track. Typically after such an event, the equalizer cannot recover until the next sequence of training symbols is received. In the TDMA systems considered here, this means that the equalizer cannot recover until the beginning of the next time slot, which begins with a known training sequence. As a result, the data in that period after the deep fade will be

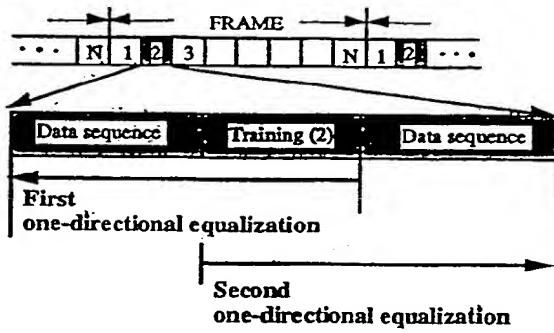


Fig. 4. One directional equalization procedure for TDMA communication systems with middle training symbols.

totally lost. For these reasons, TDMA communication systems which use one-directional equalization techniques suffer one major disadvantage: *the time slot duration must be chosen so as to keep the average number of fades per slot small*. If it is not, simply increasing signal power will not help and while interleaving with coding will help, it may be at an unacceptable cost in processing delay.

Table I shows that  $\kappa$  is equal to 0.5333 for the North American Digital Cellular TDMA system at vehicle speed equal to 60 mph. This implies that 50% of the transmitted time slots will be hit by deep fades. Under such conditions, conventional one-directional equalization techniques cannot perform well.

#### B. Bidirectional Decision Feedback Equalization Techniques

The major difference between our approach to bidirectional equalization [5] and conventional techniques is that an additional control mechanism is added to monitor the error signal, providing information on the tracking status of the equalizer. The equalization process is initiated both in the forward direction and in the reverse direction, and the error signal is used to identify the onset of a deep fade in each direction. When a deep fade is identified in either direction, the equalizer stops progress in that direction. In a single deep fade in a time slot, the result will be reliable equalization of all received signals except for the period of the deep fade itself.

All the received symbols in the current *effective time slot* are stored in a temporary buffer to allow for both forward and reverse-time processing. The algorithm, which is shown in Fig. 5, of the new approach is listed here.

- 1) Start forward equalization and monitor the error signals between the estimated symbols and quantized symbols; if  $\sum |error\ signal| \geq threshold$ , stop at instant  $N_F$  and go to step 2.
- 2) Start reverse equalization and monitor the error signals between the estimated symbols and quantized symbols; if  $\sum |error\ signal| \geq threshold$ , stop at instant  $N_B$  and go to step 3.
- 3) Estimate the location of the deep fade:

$$N_{deep} = \frac{N_F + N_B}{2} \quad (4)$$

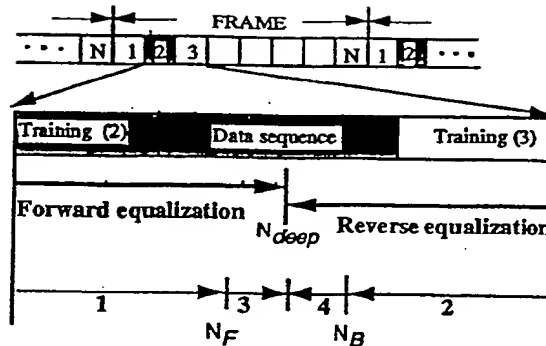


Fig. 5. Bidirectional equalization procedure for TDMA communication systems with available adjacent training symbols.

Continue forward equalization from symbol  $N_F$  to symbol  $N_{deep}$ ; go to step 4.

- 4) Continue reverse equalization from symbol  $N_B$  to symbol  $N_{deep} + 1$

The operation  $\sum |error\ signal|$  is the short-time average of the error signals, where

$$\sum |error\ signal| = \frac{1}{N_w} \sum_{j=-N_w/2}^{j=N_w/2-1} e_{n-j}^2 \quad (5)$$

and  $N_w$  is the window length of the short-time average. The threshold is a predetermined value which represents the occurrence of a deep fade within the time slot. The implementation of this algorithm is shown in the shaded area of Fig. 1. Note that this algorithm does not apply to the cases when the training symbols in the adjacent time slot are not available to the current time slot, e.g., the reverse link (from mobile to base station) of IS-54 standard.

In this algorithm, the training symbols in the adjacent time slot are assumed to be available to the current time slot. If this assumption is not valid,<sup>2</sup> and there are a number of possible training sequences for the adjacent slots, then step 2 in this algorithm should be modified to be:

"Choose any one of the possible training sequences and start reverse equalization, and monitor the error signals between the estimated symbols and quantized symbols; if  $\sum |error\ signal| \geq threshold$ , stop at this instant  $N_R$ , choose another training sequence, and retry.

If none of the possible training sequences satisfies the condition at instant  $N_R$ ,

$$\sum |error\ signal| < threshold$$

then chose the training sequence with the smallest  $\sum |error\ signal|$  and continue the reverse equalization; monitor the error signals between the estimated symbols and quantized symbols; if  $\sum |error\ signal| \geq threshold$ , stop at this instant  $N_B$ , and go to step 3."

<sup>2</sup>For example, there are six possible training sequences in the IS-54 standard, and no information is provided to the current time slot about which one is used in the adjacent time slot.

### C. Performance Evaluation of Uncoded Narrowband TDMA Systems

In this section, the applications of the new technique to the proposed North American Digital Cellular Standard, IS-54, are presented. The modulation scheme is  $\pi/4$ -shift QDPSK, and the TDMA frame structure is the same as proposed in the IS-54. Both the transmitter and receiving filters are using square root raised cosine (SRQC) pulse shaping with a rolloff factor of 0.35. There are 14 training symbols followed by 148 data symbols in a time slot. The carrier frequency is approximately 900 MHz, and the symbol duration is 41.15  $\mu$ s. The mobile radio channel is modeled as, unless specified otherwise, a two-ray channel with one symbol delay interval and two equal-strength, independent Rayleigh fading paths.

Recursive least-squares (RLS) algorithms are chosen to update the equalizer tap coefficients. The decision feedback equalizer (DFE) has three feedforward tap coefficients and one feedback tap coefficient. The forgetting factor,  $\lambda$ , is 0.85.

Since  $\pi/4$ -shift QDPSK modulation schemes is used in the transmitter, the transmitted data bits are differentially encoded. One simple way to extract information from the detected signal, which is implemented in the simulation, is to perform differential decoding and *hard decisions* according to

$$\hat{d}_{n1} = \text{sign}(\text{Re}\{Z_n\}) \quad (6)$$

$$\hat{d}_{n2} = \text{sign}(\text{Im}\{Z_n\}) \quad (7)$$

where

$$Z_n = \hat{z}_n \hat{z}_{n-1}^* \quad (8)$$

"\*" represents complex conjugate operation, and  $\hat{z}_n$  is the quantized output of the equalizer as shown in Fig. 1.

Fig. 6 illustrates the amplitude fading on a two-ray channel, plotting the log magnitude of the two paths and the error signal generated by the bidirectional equalization technique, in four different effective time slots. The value used for threshold was 0.5. This value has been found to give good results. Fig. 6 shows the following.

- 1) The equalizer converges from both directions in each time slot.
- 2) In slot one, no fade occurs and the error signal is well below the threshold.
- 3) In slot two, only one of the paths fades and the error signal again stays well below the threshold.
- 4) In slots three and four, fades occur in both paths at similar regions and no signal energy is available for the equalizer. The error signals are above the threshold, and the equalizer temporarily loses track of the channel during the fades.
- 5) In slot four,  $N_F$  is approximately 50 and  $N_B$  is approximately 84. According to (4),  $N_{\text{deep}}$  is 67, which is very close to the center of the deep fade.

Fig. 7 shows the equalizer bit error rate (BER) performance, as a function of the length of the window over which error averaging occurs, for different threshold values. This figure shows that the best performance is achieved using a threshold value of 0.6 with a window length of from 3 to 5, a threshold

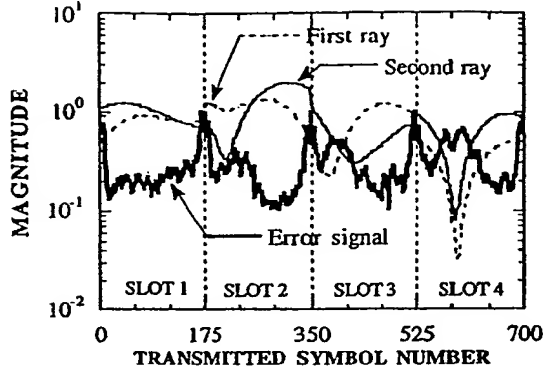


Fig. 6. Fading and error signals in four different time slots.

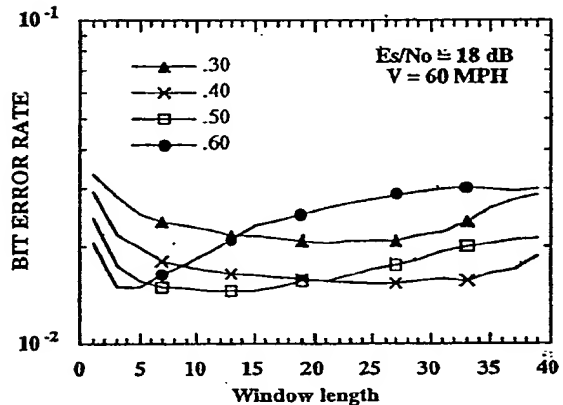


Fig. 7. BER versus window length for different thresholds {0.3, 0.4, 0.5, 0.6}.

value of 0.5 with a window length of from 7 to about 16, and a threshold value of 0.4 with a window length of about 26.

Since the threshold value of 0.5 seems to give a broad minimum, it was chosen as a reasonable compromise. In the following figures, the error threshold is set to be 0.5 and the short-time average window length is 9.

Fig. 8 shows the BER performance of one-directional, dual one-directional,<sup>3</sup> and bidirectional DFE equalization for vehicle speeds of 0.001 and 60 mph. This figure shows that the new bidirectional technique provides more than 10 dB energy gain over the conventional one-directional equalization technique at 5% BER. As a result, only 15.5 dB is required to achieve 3% BER at a vehicle speed of 60 mph, which is 6.5 dB lower than the minimum performance specification in IS-54.

We also observe that for vehicles moving at a speed of 60 mph, dual one-directional equalization has performance similar to one-directional equalization and exhibits inferior performance at low signal-to-noise ratios. This is because the error signals cannot be used as a good index for determining whether the forward or reverse equalization step provides the most reliable equalizer output. When a deep fade occurs in

<sup>3</sup>"Dual one-directional equalization" has been called "bidirectional" equalization in [15], [16]. Their schemes fall into the "dual one-directional equalization technique" category in this paper. Therefore, we choose "dual one-directional" to represent their approaches. It's also convenient for readers to distinguish our method from theirs.

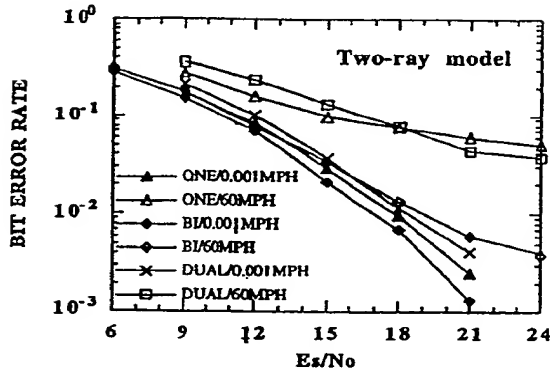


Fig. 8. BER versus  $E_s/N_0$  for different vehicle speeds with single one-directional, bidirectional, and dual one-directional decision feedback equalizers (DFE).

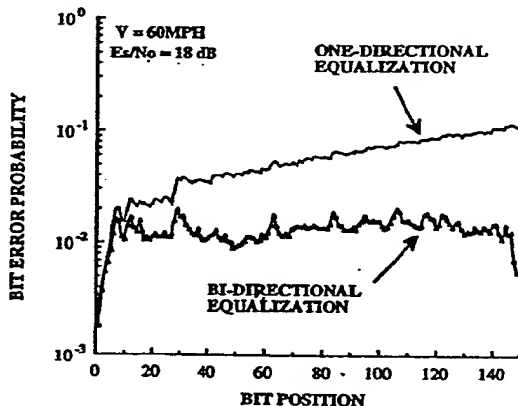


Fig. 9. BER as a function of bit position in a given time slot with one-directional and bidirectional DFE.

the middle of a time slot, the equalizer may lock up during both the forward and reverse equalization procedures. This actually occurred in slot 4 of Fig. 6 during our testing. When the equalizer locked up, the error signals dropped to zero.

Fig. 9 shows the BER as a function of bit position in a given time slot for one-directional and bidirectional DFE equalization. In one-directional equalization, the BER is a nondecreasing function of bit position. This is because the divergence of the one-directional equalizer at any point in the time slot will affect the correctness of all the subsequent received symbols, but not any of the previously received symbols.

In the previous discussion, it was noted that the bidirectional equalization technique can estimate the location of deep fades and, as a result, can limit the divergence of the equalizer to a very short period near the occurrence of the deep fade only. As a result, uniform BER is achieved over the duration of the time slot, except in the region near the beginning of the tracking mode.

Fig. 10 shows the BER performance of the conventional MLSE and  $M$  algorithm equalizers and the newly proposed bidirectional DFE equalization at a vehicle speed equal to 60 mph. Both MLSE and  $M$  algorithm equalizers use the same channel tracking/estimation technique discussed in [10].

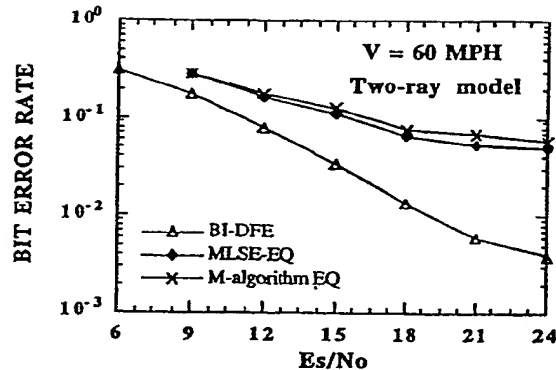


Fig. 10. Performance comparison: MLSE equalizer,  $M$  algorithm, and bidirectional DFE.

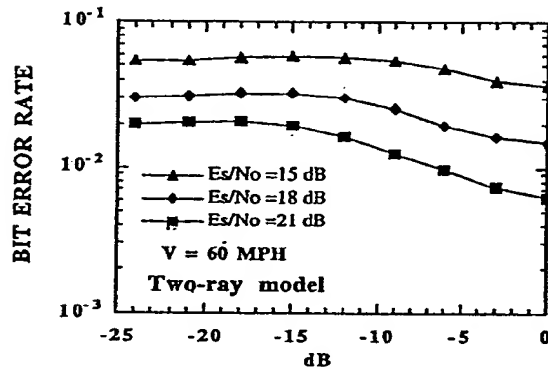


Fig. 11. BER for a two-ray model with unequal receiving power, where the  $x$  axis is the number of receiving powers (in terms of dB) of the second ray less than the receiving power of the first ray.

The tracking algorithm is RLS with the same forgetting factor as used in the bidirectional DFE, which is equal to 0.85. In general,  $M < S$ , where  $S$  is the number of the states of the channels. Here, we choose  $M$  equal to 3 in the  $M$  algorithm, as suggested in [12]. We observe that MLSE and  $M$  algorithm have performance similar to one-directional DFE.<sup>4</sup> This is because the occurrences of deep fades, as in the case of one-directional DFE, will cause the divergence of the tracking algorithms used in both equalizers.

Fig. 11 shows the sensitivity of the proposed bidirectional technique to variations from the equal power assumption in the two-ray model. This figure shows that as the received power gets concentrated into only one of the rays, the diversity advantage gained through the presence of two independently fading channels decreases.

Fig. 12 shows the sensitivity of the proposed techniques to different sampling points within one symbol duration. It is observed that  $\pm 5 \mu s$  timing error is still acceptable.

Fig. 13 shows the BER performance of the proposed bidirectional technique to different delay intervals (fraction of symbol interval) in the two-ray model for different vehicle speeds of 0.001 and 60 mph. We observe that for vehicles

<sup>4</sup>It has been reported in [11] that a better performance can be achieved with the MLSE-type equalizer. However, no specific algorithm is discussed in the paper.

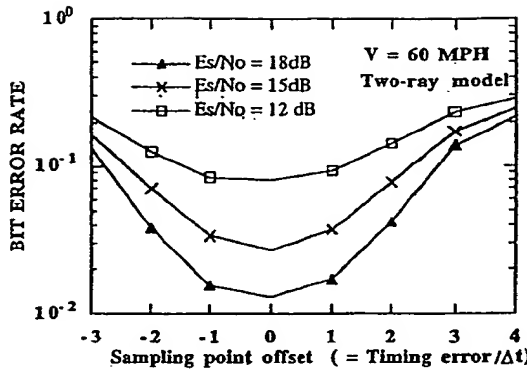
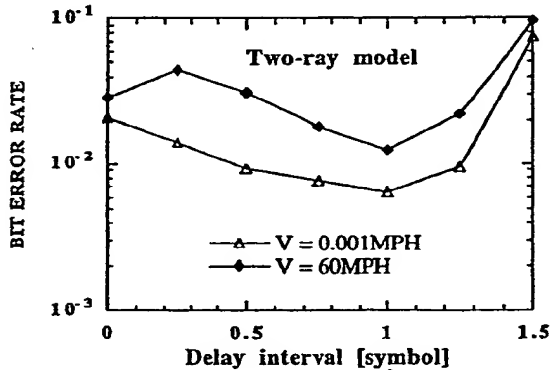
Fig. 12. BER versus sampling error  $n\Delta t$ , where  $\Delta t$  is  $T_0/8 = 5.02 \mu s$ .

Fig. 13. BER versus different delay intervals for a two-ray model.

moving at a speed of 60 mph, the performance degrades with increasing delay up to approximately 1/4 symbol interval and then improves to one symbol interval. The performance starts to degrade again when the delay interval is larger than one symbol. This performance changing can be explained as follows.

- 1) The filtering operation introduces intersymbol interference, from symbols outside the equalizer control range. Around the 1/4 symbol interval, the amount of ISI reaches its maximum.
- 2) Above one symbol period, the delay interval is larger than the equalizer control range. Therefore, the performance starts to degrade again.

Fig. 14 shows the BER as a function of the number of training symbols. This figure shows that the performance is significantly improved by increasing the number of training symbols from 4 to 7, but that the performance cannot be further improved by using more than seven. Thus, the 14 training symbols specified in the IS-54 Standard are more than adequate for the bidirectional equalizer.

#### D. Complexity Issues

The complexity of the proposed techniques in terms of the number of additions, multiplications, and divisions per iteration is shown in Table II. The number of operations required for the algorithm is determined by assuming that the multichannel lattice structure is used [7].

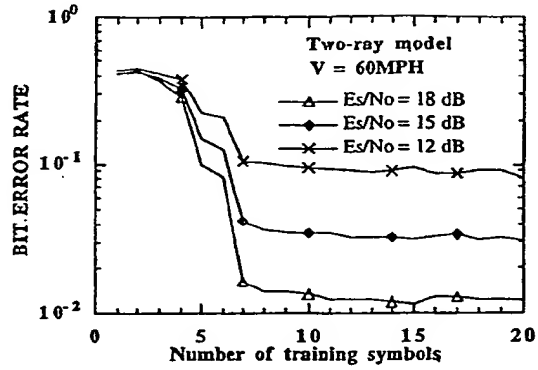


Fig. 14. BER versus number of training symbols.

TABLE II  
COMPLEXITY COMPARISON OF THE PROPOSED ADAPTIVE DFE, WHERE  $M_1$  IS THE NUMBER OF FEEDFORWARD TAPS AND  $M_2$  IS THE NUMBER OF FEEDBACK TAPS

RLS algorithm	operations/symbol	$M_1 = 3, M_2 = 1$
Addition	$9M_1 + 34M_2 - 27$	20
Multiplication	$19M_1 + 44M_2 - 45$	56
Division	$2M_1$	6

The total number of instructions executed per second executed by the DSP processor can be calculated as follows:

$$(\text{add} + \text{mul} + \text{div}) \times \text{effective symbols/slot} \times \text{slot/seconds}. \quad (9)$$

The effective number of symbols per slot should include the training symbols in the adjacent time slot and, when the equalizer must try several different training sequences, this must be included in (9).

In general, addition and multiplication operations can be achieved within one instruction cycle by most state-of-art digital signal processors. If it is further assumed that one division operation can be finished within 10 instruction cycles, then the number of operations required for bidirectional equalization applied to IS-54 as described, expressed in millions of operations per second, is about 6.8 MIPS.

This result indicates that less than 7 MIPS are required for a bidirectional equalizer applied to an IS-54 mobile. This level of processing power is well within the capabilities of currently available general-purpose programmable DSP chips, and represents a small fraction of the total processing power required for the implementation of an IS-54 mobile.

#### V. SOFT-DECISION DECODING TECHNIQUES FOR THE EQUALIZED RADIO CHANNELS

If convolutional encoding is used to improve system performance at the receiver, the inputs to the Viterbi decoder must be derived from the equalizer output. A fundamental problem encountered in designing high-performance decoding techniques for use with IS-54 is that the interleaving process interleaves bits, while the channel symbols each represent two bits. However, the two bits contained in a channel symbol will be separated by the deinterleaver when they are passed to

the decoder. For this reason, it is not possible to pass channel symbol soft decisions to the decoder. Instead, it is necessary to generate decisions on individual bits to send to the decoder.

One approach is to make *hard decisions* on the equalizer output, i.e., quantize to one bit per decision. Only the sign bits are preserved by this operation, so some information is lost. A better approach is to make *soft decisions* which preserve the information available in the unquantized outputs from the equalizer.

In the following sections, we will derive the equivalent equalized channel model, which is necessary in order to understand the statistic of each unquantized output from the equalizer so as to derive the soft-decision metrics for the decoder.

#### A. Bidirectionally Equalized Mobile Radio Channels

Without loss generality, let us consider a special case in which the DFE, with three forward taps and one feedback tap, operates in a slow fading channel with one symbol delay spread. This combination,  $M_1 = 3$ ,  $M_2 = 1$  gives an acceptable performance in an uncoded IS-54 channel, which was shown in the previous section. From (1), the received signal is

$$r_n = h_1 a_n + h_2 a_{n-1} + \eta_n. \quad (10)$$

It has been shown that the tap coefficients will converge to different optimum values according to the minimum and non-minimum phase conditions at high signal-to-noise ratios [17]. The nonminimum phase condition for the forward equalization will become the minimum phase conditions for the reverse equalization and vice versa.

- *Forward equalization:*

- 1) *Minimum phase condition:*

If it is assumed that  $|h_1| \gg |h_2|$ , then the tap coefficients will converge to

$$\begin{aligned} \alpha_{-2} &\approx 0, & \alpha_{-1} &\approx 0, \\ \alpha_0 &\approx h_2^*/|h_2|^2, & \beta_0 &\approx -h_1 h_2^*/|h_2|^2. \end{aligned}$$

The equalized channel is

$$r_n = a_n + \eta_n/h_1. \quad (11)$$

- 2) *Nonminimum phase condition:*

If it is assumed that  $|h_2| \gg |h_1|$ , then the tap coefficients will converge to

$$\begin{aligned} \alpha_{-2} &\approx \frac{h_1}{h_2} \frac{(1 - (h_1/h_2)^2)}{h_2}, \\ \alpha_{-1} &\approx \frac{(1 - (h_1/h_2)^2)}{h_2}, \\ \alpha_0 &\approx \frac{h_1^*}{|h_2|^2}, & \beta_0 &\approx \left(\frac{h_1}{h_2}\right)^*. \end{aligned}$$

The equalized channel is

$$r_n = a_n + \zeta_n \quad (12)$$

where

$$\begin{aligned} \zeta_n = & -\left(\frac{h_1}{h_2}\right)^2 \left(1 - (h_1/h_2)^2\right) a_{n+2} \\ & + \frac{h_1^*}{|h_2|^2} \eta_n + \frac{\left(1 - (h_1/h_2)^2\right)}{h_2} \eta_{n+1} \\ & - \frac{h_1}{h_2} \frac{\left(1 - (h_1/h_2)^2\right)}{h_2} \eta_{n+2} \end{aligned} \quad (13)$$

the equivalent noise.

In (13), the first term is the uncancelled future ISI, which is very small under the assumption that  $|h_2| \gg |h_1|$ .

- *Reverse equalization:*

All the equations listed above apply for reverse equalization, with  $h_1$  replaced by  $h_2$  and  $h_2$  replaced by  $h_1$ .

Under these assumptions, and under the minimum phase conditions for both forward and reverse equalization, the equalized channel is equivalent to a unit-gain channel with additive white Gaussian noise divided by a complex Gaussian random variable. Under the nonminimum phase condition, the equalized channel is equivalent to the sum of a unit-gain channel with the sum of additive Gaussian noises plus uncancelled future ISI, weighted by the forward tap coefficients. These results apply for a two-ray model when one ray is much stronger than the other. When this restriction does not hold, the analysis is much less straightforward than that presented. However, our simulation experience shows that use of soft-decision metrics which follow from this analysis provide significant performance gains when the two rays are of equivalent strength.

#### B. Bit Likelihood Soft Decisions

In [14], an algorithm to generate soft-decision metrics for the Viterbi decoder is proposed. The algorithm, however, is suboptimal due to the fact that only two (the first- and second-closest phase to the received phase) of four possible phases are considered.

A better approach is to use maximum-likelihood metrics as soft decisions. For  $\pi/4$ -shift QDPSK modulation schemes, the current output bits depend on the current and previous estimated symbols. The log likelihood ratio for the *I* and *Q* component is:

$$L_n(I \text{ or } Q) = \log \left( \frac{\text{Joint pdf of } (\tilde{z}_n, \tilde{z}_{n-1}/b_n(I \text{ or } Q) = 0)}{\text{Joint pdf of } (\tilde{z}_n, \tilde{z}_{n-1}/b_n(I \text{ or } Q) = 1)} \right) \quad (14)$$

where  $\tilde{z}_n$  is the unquantized output of the equalizer as given by (23), which is derived in the Appendix.

From (11) and (12), we observe that, at high signal-to-noise ratio, the conditional joint pdf of

$$(\tilde{z}_n, \tilde{z}_{n-1}/b_n(I \text{ or } Q) = 0)$$

is Gaussian, provided the channel is constant over two consecutive symbol periods, the uncancelled ISI is small, and either  $|h_1| \gg |h_2|$  or  $|h_2| \gg |h_1|$ . By using Table III and the Gaussian assumption, which is valid only under

certain conditions, the bit log-likelihood ratio for the  $I$  and  $Q$  components can be shown as:

$$\begin{aligned}
 L(I) = & \log \left( \exp \left\{ -\frac{1}{2\sigma_n^2} \left[ (x_n - 1)^2 + (y_n - 1)^2 \right. \right. \right. \\
 & \quad \left. \left. \left. + (y_{n-1} + 1)^2 \right] \right\} \right. \\
 & + \exp \left\{ -\frac{1}{2\sigma_n^2} \left[ (x_n - 1)^2 + (y_n + 1)^2 \right. \right. \\
 & \quad \left. \left. + (x_{n-1} + 1)^2 \right] \right\} \\
 & + \exp \left\{ -\frac{1}{2\sigma_n^2} \left[ (x_n + 1)^2 + (y_n + 1)^2 \right. \right. \\
 & \quad \left. \left. + (y_{n-1} - 1)^2 \right] \right\} \\
 & + \exp \left\{ -\frac{1}{2\sigma_n^2} \left[ (x_n + 1)^2 + (y_n - 1)^2 \right. \right. \\
 & \quad \left. \left. + (x_{n-1} - 1)^2 \right] \right\} \\
 & - \log \left( \exp \left\{ -\frac{1}{2\sigma_n^2} \left[ (x_n - 1)^2 + (y_n - 1)^2 \right. \right. \\
 & \quad \left. \left. + (y_{n-1} - 1)^2 \right] \right\} \right. \\
 & + \exp \left\{ -\frac{1}{2\sigma_n^2} \left[ (x_n - 1)^2 + (y_n + 1)^2 \right. \right. \\
 & \quad \left. \left. + (x_{n-1} - 1)^2 \right] \right\} \\
 & + \exp \left\{ -\frac{1}{2\sigma_n^2} \left[ (x_n + 1)^2 + (y_n + 1)^2 \right. \right. \\
 & \quad \left. \left. + (y_{n-1} + 1)^2 \right] \right\} \\
 & + \exp \left\{ -\frac{1}{2\sigma_n^2} \left[ (x_n + 1)^2 + (y_n - 1)^2 \right. \right. \\
 & \quad \left. \left. + (x_{n-1} + 1)^2 \right] \right\} \quad (15)
 \end{aligned}$$

and

$$\begin{aligned}
 L(Q) = & \log \left( \exp \left\{ -\frac{1}{2\sigma_n^2} \left[ (x_n - 1)^2 + (y_n - 1)^2 \right. \right. \right. \\
 & \quad \left. \left. \left. + (x_{n-1} + 1)^2 \right] \right\} \right. \\
 & + \exp \left\{ -\frac{1}{2\sigma_n^2} \left[ (x_n - 1)^2 + (y_n + 1)^2 \right. \right. \\
 & \quad \left. \left. + (y_{n-1} - 1)^2 \right] \right\} \\
 & + \exp \left\{ -\frac{1}{2\sigma_n^2} \left[ (x_n + 1)^2 + (y_n + 1)^2 \right. \right. \\
 & \quad \left. \left. + (x_{n-1} - 1)^2 \right] \right\} \\
 & + \exp \left\{ -\frac{1}{2\sigma_n^2} \left[ (x_n + 1)^2 + (y_n - 1)^2 \right. \right. \quad (16)
 \end{aligned}$$

TABLE III  
 $\pi/4$  SHIFT QDPSK MODULATION DIFFERENTIAL ENCODING TABLE

Previous state	Present state				
	input vector	0 0	0 1	1 1	1 0
output change $\Delta\theta$	$\pi/4$	$3\pi/4$	$-3\pi/4$	$-\pi/4$	
0 0		0 0	0 1	1 1	1 0
0 1		0 1	1 1	1 0	0 0
1 1		1 1	1 0	0 0	0 1
1 0		1 0	0 0	0 1	1 1

$$\begin{aligned}
 & \left. + (y_{n-1} + 1)^2 \right] \} \right) \\
 & - \log \left( \exp \left\{ -\frac{1}{2\sigma_n^2} \left[ (x_n - 1)^2 + (y_n - 1)^2 \right. \right. \\
 & \quad \left. \left. + (x_{n-1} - 1)^2 \right] \right\} \right. \\
 & + \exp \left\{ -\frac{1}{2\sigma_n^2} \left[ (x_n - 1)^2 + (y_n + 1)^2 \right. \right. \\
 & \quad \left. \left. + (y_{n-1} + 1)^2 \right] \right\} \\
 & + \exp \left\{ -\frac{1}{2\sigma_n^2} \left[ (x_n + 1)^2 + (y_n + 1)^2 \right. \right. \\
 & \quad \left. \left. + (x_{n-1} + 1)^2 \right] \right\} \\
 & + \exp \left\{ -\frac{1}{2\sigma_n^2} \left[ (x_n + 1)^2 + (y_n - 1)^2 \right. \right. \\
 & \quad \left. \left. + (y_{n-1} - 1)^2 \right] \right\} \quad (16)
 \end{aligned}$$

where

$$\tilde{z}_n = (x_n, y_n)$$

and  $\sigma_n^2$  is the instantaneous noise power from time  $n - 1$  to  $n$ , which can be derived from the error signal. Since exponential operations in (15) and (16) demand high computation power, further simplification for both equations is required for practical use.

### C. Instantaneous Noise Power Estimation

From (11) and (12), we know that the equalized channel is a unit-gain channel with additive white noise divided by a complex Gaussian random variable. The instantaneous noise power is  $E(\eta_n^2)/E(h_1^2)$  for the forward equalization and  $E(\eta_n^2)/E(h_2^2)$  for the reverse equalization under the assumption of minimum phase condition. The instantaneous noise power is  $E(\zeta_n^2)$ , where  $\zeta$  is defined in (13), under the assumption of nonminimum phase condition.

From the equalizer structure, (11) and (12), we know that the simplest way to derive an estimate of these values is based on the error signals  $e_n$ . To get an estimate of the noise power, a short-term average of the equalizer error signal power is

computed

$$\tilde{\sigma}_n^2 = \frac{1}{N_w} \sum_{j=-N_w/2}^{j=N_w/2-1} e_{n-j}^2 \quad (17)$$

where  $N_w$  is the window length of the short-time average, which should depend on the forgetting factor  $\lambda$  used in the adaptive algorithm of the system. For example, if  $\lambda = 0.85$ , then

$$N_w = \frac{1}{1 - \lambda} \sim 7$$

is a good choice.

This error estimate is accurate under the condition that only a small fraction of the equalizer decisions are in error. This assumption does not hold for all channel conditions. In particular, the DFE may diverge or lock up when a deep fade occurs, resulting in an error signal which is either very large or goes to zero. Under such conditions, the error signal is not sufficiently reliable to derive the noise power.

A more robust estimate of the noise power, which gives good performance over the full range of channel conditions, is to use the short-term average of the equalizer error only when it falls into some intermediate range, and to limit its values when it falls outside of this range. The following limiting form has been found to provide good results:

$$\tilde{\sigma}_n^2 = \begin{cases} 0.2 & \text{if } \tilde{\sigma}_n^2 < 0.2 \\ 0.5 & \text{if } \tilde{\sigma}_n^2 > 0.5 \\ \tilde{\sigma}_n^2 & \text{otherwise.} \end{cases} \quad (18)$$

#### D. Performance Evaluation of Coded and Equalized Narrowband TDMA Systems

This section presents simulation results of the previously discussed techniques to the forward link of the proposed Northern American Digital Cellular Communication System. The TDMA frame structure, which is used here, is the same as proposed in IS-54.

The input bits are divided into two classes. There are Class 1 bits, which are input to the convolutional coder. The rest of the bits are Class 2 bits and are uncoded. After interleaving, the source bits (uncoded and encoded bits) are modulated by a  $\pi/4$ -shift QDPSK function and then sent to the communication channel. The equalized channel is a combination of the radio channel and a bidirectional decision feedback equalizer.

Fig. 15 shows the histogram of the  $I$  components of the maximum-likelihood soft decision without data modulation; that is  $b_n L_n(I)$  at vehicle speed equal to 60 mph. At a low signal-to-noise ratio, 0 dB, two spikes (at 1.32 and -1.32) are observed. These two spikes indicate that the equalizer occasionally "locks up" that is, the feedforward tap coefficients of the equalizer converge to zero and the feedback tap coefficients converge to  $e^\phi$ , where  $\phi \in \{\pi/4, 3\pi/4, -3\pi/4, \pi/4\}$ . The soft decisions, calculated from (15) and (16), are 1.32 when  $\phi = \pi/4$  or  $-\pi/4$  and -1.32 when  $\phi = 3\pi/4$  or  $-3\pi/4$ . Note that this "lockup" condition is stable. At higher signal-to-noise ratios, the spikes disappear and the soft-decision metrics

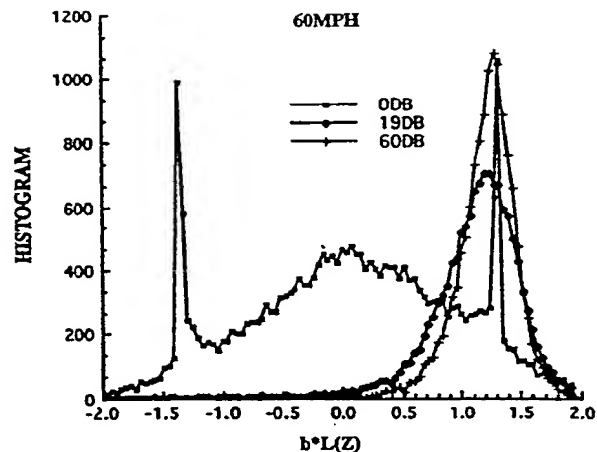


Fig. 15. Histogram for soft decision outputs without data modulation.

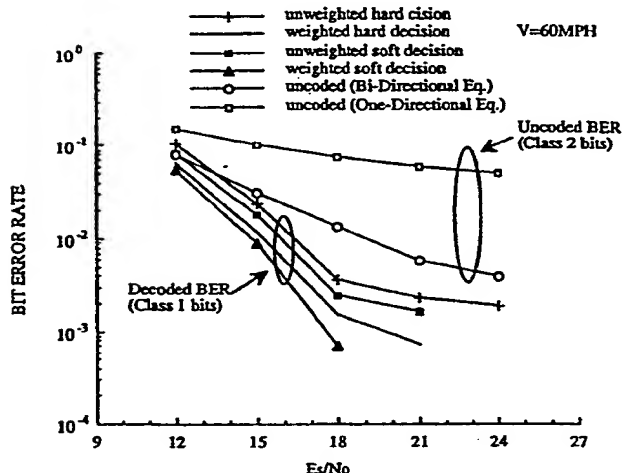


Fig. 16. BER versus  $E_s/N_o$  for different soft and hard decision schemes.

are grouped around 1.32, the metric which results when the symbols differ by  $\pm\pi/4$  or  $\pm3\pi/4$ .

Fig. 16 shows the Class 1 and 2 bit error rate curves for different signal-to-noise ratios. The metrics, used in the curve marked "unweighted hard decision," are conventional hard decisions. In the curve marked "weighted hard decision," the metrics are hard decisions divided by  $\tilde{\sigma}_n^2$ , the noise power. In the curve marked "unweighted soft decision," the metrics are derived from (15) and (16) with  $\tilde{\sigma}_n^2 = 1$ ; in the curve marked "weighted soft decision"  $\tilde{\sigma}_n^2$  is equal to (18). Weighted soft-decision decoding is observed to be about 2 dB better than unweighted hard decision decoding at 1% BER. We also observe that scaling by a short-term error estimate provides more gain than use of the exact maximum-likelihood QDPSK metric.

## VI. CONCLUSIONS

This paper proposes a novel low-complexity adaptive equalization technique which uses information in the adjacent time slot in a time division multiple access (TDMA) system to

improve the digital transmission system performance over time-varying land mobile radio channels.

Application of the new technique to the forward link of the proposed Telecommunications Industry Association (TIA) Northern American Digital Cellular Standard (IS-54) was investigated. The simulation results showed that, without diversity and with very low complexity, only 15.5 dB of signal-to-noise power ratio is needed to achieve 3% BER at a vehicle speed equal to 60 mph, which is 6.5 dB lower than the IS-54 specification.

An equivalent equalized land mobile radio channel model and the analytical solution for the optimal bit likelihood calculation for  $\pi/4$ -shift QDPSK modulation were also derived under certain channel conditions. The results were used as soft decisions for the convolutional decoder. The likelihood calculation requires an estimate of the instantaneous noise variance. A good estimate may be derived from the equalizer error signal, but care must be taken to avoid use of the error signal when the equalizer is not tracking the channel. This approach gives a 1% decoded BER with 2 dB less power than that required for hard decisions.

#### APPENDIX

In this Appendix, an equivalent model for the equalized mobile radio channel is derived, based on the assumptions that the channel fades slowly and that correct decisions are used to adapt the equalizer coefficients.

First, consider the forward equalization operation. The estimated symbol at time  $n$ , unquantized output of the equalizer, is

$$\tilde{z}_n = \sum_{i=-M_1}^0 \alpha_i r_{n-i} - \sum_{j=1}^{M_2} \beta_j \hat{z}_{n-j} \quad (19)$$

where  $M_1 + 1$  is the number of feedforward taps,  $M_2$  is the number of feedback taps,  $\hat{z}_k$  is the quantized output of the equalizer,  $\alpha_i$  are the feedforward tap coefficients, and  $\beta_j$  are the feedback tap coefficients. The error signal  $e_n$  is defined as

$$e_n = \tilde{z}_n - \hat{z}_n. \quad (20)$$

Under the assumption of correct decisions,  $\hat{z}_{n-j}$  is equal to  $a_{n-j}$ . Substituting (1) into (19) leads to

$$\tilde{z}_n = \sum_{i=-M_1}^L H_{i,n} a_{n-i} + v_n - \sum_{j=1}^{M_2} \beta_j a_{n-j} \quad (21)$$

where  $L$  is the length of the channel response as defined in (1)

$$H_{i,n} = \sum_{m=-M_1}^0 \alpha_m h_{i-m, n-m}$$

and

$$v_n = \sum_{i=-M_1}^0 \alpha_i \eta_{n-i}.$$

If

$$g_{i,n} = \begin{cases} H_{i,n} - \beta_i & i = 1, \dots, M_2 \\ H_{i,n} & \text{otherwise} \end{cases} \quad (22)$$

then (21) can be further simplified to be

$$\tilde{z}_n = \sum_{i=-M_1}^L g_{i,n} a_{n-i} + v_n \quad (23)$$

where  $g_i$  is the equivalent channel impulse response.

The optimal setting of the tap coefficients can be derived based on the minimum mean squared error (MMSE) criterion. From the orthogonality principle, we also know that the error signal should be orthogonal to the received signal in the forward filter and to the decisions in the feedback filter:

$$E\{\tau_{n-i} e_n^*\} = 0 \quad i = 0, \dots, M_1 \quad n = 0, 1, \dots \quad (24)$$

$$E\{a_{n-j} e_n^*\} = 0 \quad j = 1, \dots, M_2 \quad (25)$$

where  $e_n$  is defined in (20). It has been derived that the optimal setting of tap coefficients satisfies the following set of linear equations:

$$\sum_{i=0}^{M_1} \alpha_i \Xi_{m,j}^n = h_m^* \quad m = 0, \dots, M_1 \quad (26)$$

$$\sum_{i=0}^{M_1} \alpha_i h_{m+j} = \beta_m \quad m = 0, \dots, M_1 \quad (27)$$

where

$$\Xi_{m,j} = \sum_{u=0}^m h_u^* h_{u+j-m} + \phi_{j-m} \quad (28)$$

$$\phi_k = \begin{cases} N_0 & k = 0 \\ 0 & \text{otherwise.} \end{cases} \quad (29)$$

#### ACKNOWLEDGMENT

The authors thank Dr. D. Fye for his encouragement of this work and the anonymous reviewers for their many constructive comments and suggestions.

#### REFERENCES

- [1] M. R. L. Hodges, "The GSM radio interface," *Brit. Telecom Technol.*, vol. 8 no. 1, pp. 31–43, Jan. 1990.
- [2] TR45.3 IS-54, Dual-Mode Mobile Station—Base Station Compatibility Standard.
- [3] "CDMA cellular—The next generation," PacTel Cell. and Qualcomm, Inc., Nov. 1989.
- [4] Y. J. Liu and J. Ketchum, "Performance of antenna diversity and decision feedback equalizers in narrowband digital cellular systems," *Electron. Lett.*, vol. 27, pp. 953–955, 1991.
- [5] Y. J. Liu, "Bidirectional equalization technique for TDMA communication systems over land mobile radio channels," *IEEE GLOBECOMM'91*, Phoenix, AZ, 1991, pp. 41.1–41.5.
- [6] W. C. Jakes, Jr., *Microwave Mobile Communications*. New York: Wiley, 1974.
- [7] F. Ling and J. G. Proakis, "Adaptive lattice decision-feedback equalizers—Their performance and application to time-variant multipath channels," *IEEE Trans. Commun.*, vol. COM-33, no. 4, pp. 348–356, Apr. 1985.
- [8] E. Eleftheriou and D. D. Falconer, "Adaptive equalization techniques for HF channels," *IEEE J. Select Areas Commun.*, vol. SAC-5, no. 2, pp. 238–247, Feb. 1987.
- [9] H. Shiino, N. Yamaguchi, and Y. Shoji, "Performance of an adaptive maximum-likelihood receiver for fast fading multipath channel," in *Proc. 42nd IEEE Vehic. Technol. Conf.*, Denver, CO, 1992, pp. 380–383.
- [10] E. Dahlman, "New adaptive Viterbi detector for fast-fading mobile radio channels," *Electron. Lett.*, vol. 26, pp. 1572–1573, 1990.
- [11] G. Larsson, B. Gudmundson, and K. Raith, "Receiver performance for the North American digital cellular system," in *Proc. 41st IEEE Vehic. Technol. Conf.*, St. Louis, MO, 1991, pp. 1–6.

- [12] A. Baier and G. Heinrich, "Performance of M-algorithm MLSE equalizer in frequency-selective fading mobile radio channels," in *Proc. IEEE ICC '89*, Boston, MA, 1989, pp. 281-285.
- [13] R. Mehlhan and H. Meyr, "Soft output M-algorithm equalizer and trellis-coded modulation for mobile radio communication," in *Proc. 42nd IEEE Vehic. Technol. Conf.*, Denver, CO, 1992, pp. 586-591.
- [14] M. Abe, H. Shiino, and Y. Shoji, "Analysis on bit-error characteristics of channel codec in digital mobile communications systems," in *Proc. 41st IEEE Vehic. Technol. Conf.*, St. Louis, MO, 1991, pp. 17-22.
- [15] H. Suzuki, "Performance of a new adaptive diversity-equalization for digital mobile radio," *Electron. Lett.*, vol. 26, pp. 626-627, 1990.
- [16] Y. Kamio and S. Sampei, "Performance of reduced complexity DFE using bidirectional equalization in land mobile communication," in *Proc. 42nd IEEE Vehic. Technol. Conf.*, Denver, CO, 1992, pp. 372-375.
- [17] H. Suzuki, T. Ueda, and A. Higashi, "High bit-rate digital mobile radio transmission with a decision feedback equalizer," in *Proc. IEEE ICC '89*, Boston, MA, 1989, pp. 6.1.1-6.1.5.



**Yow-Jong Liu** (S'87-M'89) was born in Kaohsiung, Taiwan, in 1958. He received the B.Sc. and M.Sc. degrees in electronics engineering from National Chiao Tung University, Taiwan, R.O.C., in 1980 and 1982, respectively, and the Ph.D. degree in electrical engineering from the University of California, Los Angeles, in 1989. He worked for the Technology Group, Los Angeles, CA, from 1988 to 1989. Since August 1989, he has been with GTE Laboratories, Waltham, MA, where his work is primarily on mobile and portable communications. His current research interests include performance analysis of multiple access techniques, digital wireless communication systems design, and DSP implementation of signal processing algorithms.



**Mark Wallace** was born in Cleveland, OH, on October 7, 1956. He received the Ph.D. degree from the University of Illinois, Urbana-Champaign, in 1982.

From 1982 to 1990, he was with Signatron, Inc. and worked mainly in the area of troposcatter communications. Since 1990, he has been with the Mobile Systems Department of GTE Laboratories, where he is concerned with various aspects of mobile communications.



**John W. Ketchum** received the Ph.D. degree in electrical engineering from Northeastern University, Boston, MA, in 1982.

From 1982 to 1985, he was an Assistant Professor of Electrical Engineering at Northeastern University, teaching graduate and undergraduate courses in communications-related areas and performing sponsored research in the areas of adaptive signal processing and digital communication. Since 1985, he has been a Principal Member of Technical Staff at GTE Laboratories, where his research interests and responsibilities have encompassed various topics in digital communications, with an almost exclusive focus on mobile communications since 1987. His current research interests include analysis and simulation of mobile and personal communication systems, and packet data access techniques for mobile systems.

**This Page is Inserted by IFW Indexing and Scanning  
Operations and is not part of the Official Record**

**BEST AVAILABLE IMAGES**

Defective images within this document are accurate representations of the original documents submitted by the applicant.

Defects in the images include but are not limited to the items checked:

- BLACK BORDERS**
- IMAGE CUT OFF AT TOP, BOTTOM OR SIDES**
- FADED TEXT OR DRAWING**
- BLURRED OR ILLEGIBLE TEXT OR DRAWING**
- SKEWED/SLANTED IMAGES**
- COLOR OR BLACK AND WHITE PHOTOGRAPHS**
- GRAY SCALE DOCUMENTS**
- LINES OR MARKS ON ORIGINAL DOCUMENT**
- REFERENCE(S) OR EXHIBIT(S) SUBMITTED ARE POOR QUALITY**
- OTHER:** \_\_\_\_\_

**IMAGES ARE BEST AVAILABLE COPY.**

**As rescanning these documents will not correct the image problems checked, please do not report these problems to the IFW Image Problem Mailbox.**

THIS PAGE BLANK (USPTO)